

THE STRENGTH OF SOLID PRISMATIC
MEMBERS IN TORSION

by

HASEEB AHMED KHAN

B. E. (Civil), University of Karachi, Karachi, 1966

A MASTER'S THESIS

submitted in partial fulfillment of the

requirements for the degree

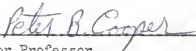
MASTER OF SCIENCE

Department of Civil Engineering

KANSAS STATE UNIVERSITY
Manhattan, Kansas

1969

Approved by:


Major Professor

LD
2668
74
1969
K53

TABLE OF CONTENTS

	Page
1 INTRODUCTION	1
1.1 GENERAL	1
1.2 PURPOSE AND SCOPE OF RESEARCH	1
2 LITERATURE SURVEY	2
2.1 HISTORICAL BACKGROUND	2
2.2 ELASTIC SOLUTIONS TO TORSIONAL PROBLEMS FOR SOLID PRISMATIC MEMBERS	4
(a) Circular Cross Sections	8
(b) Rectangular Cross Sections	13
(c) Square Cross Sections	17
(d) Summary	17
2.3 PLASTIC SOLUTIONS TO TORSIONAL PROBLEMS FOR SOLID PRISMATIC MEMBERS	17
(a) Circular Cross Sections	22
(b) Rectangular Cross Section	24
(c) Square Cross Section	25
(d) Summary	26
3 EXPERIMENTAL PROGRAM	26
3.1 GENERAL	26
3.2 DESIGN OF TENSILE TEST EXPERIMENTS	26
(a) Test Specimens	26
(b) Apparatus Used	29
(c) Experimental Procedure	29
3.3 DESIGN OF TORSION TEST EXPERIMENTS	36
(a) Test Specimens	36
(b) Apparatus Used	38
(c) Experimental Procedure	40
4 PRESENTATION AND INTERPRETATION OF DATA	42
4.1 MATERIAL PROPERTIES FROM TENSION TESTS	42
4.2 TORQUE-TWIST CURVES	46

TABLE OF CONTENTS (Contd.)

	Page
4.3 TORQUE-STRESS CURVE	69
4.4 CORRELATION OF THEORETICAL AND EXPERIMENTAL TORQUES	72
4.5 CORRELATION OF THEORETICAL AND EXPERIMENTAL SHEAR STRESSES.	75
5 CONCLUSIONS	77
6 RECOMMENDATIONS FOR FURTHER RESEARCH.	78
7 ACKNOWLEDGEMENT	79
8 REFERENCES.	80

1 INTRODUCTION

1.1 GENERAL

In the design of machinery and some structures, the problem of transmitting a torque (a couple) from one plane to a parallel plane is frequently encountered. The simplest device to accomplish this function is a shaft. Shafts are found in the form of Line Shafts, Head Shafts, Crank Shafts and ship and aeroplane propeller shafts. Twisting or Torsion is generally, although not exclusively, encountered in machine design.

Torsion is the term applied to the twisting action in a bar that is subjected to the effect of externally applied torques or twisting moments acting in planes normal to the axis of the bar.

Transmission shafting may also be subjected to bending owing to the weight of pulleys, motors or other equipment supported by the shaft. Problems involving loading that produces combined stresses are not considered in this discussion. The members are subjected only to torsion.

Solutions to torsion problems fall into the following categories according to the types of members transmitting the torque:

- (i) Solid prismatic members.
- (ii) Solid non-prismatic members.
- (iii) Hollow prismatic members.
- (iv) Hollow non-prismatic members.

1.2 PURPOSE AND SCOPE OF RESEARCH

The objective of the investigation was to study experimentally the behavior of solid prismatic bars subjected to pure torsion and to compare the experimental results with existing analytical solutions. Both elastic and plastic behavior were studied.

The research was limited in scope to solid, prismatic steel members subjected to pure torsion. The following cross sections were studied:

- (i) Circular
- (ii) Rectangular
- (iii) Square

2 LITERATURE SURVEY

2.1 HISTORICAL BACKGROUND

The elastic study of torsional problems dates as far back as the Eighteenth Century, when Coulomb's theory for a circular cross section was published in "Histoire de L'academie" in 1784.¹

Navier, in 1864, tried to correlate this theory with members having non-circular cross sections.² He deduced an incorrect relationship and came to the erroneous conclusion that, for a given torque, the angle of twist is inversely proportional to the centroidal moment of inertia of the cross section, and, that the maximum shear stress occurs at points most remote from the centroid of the cross section. In contrast to Navier's theory, it was later shown experimentally that when non-circular prismatic bars are twisted, initially plane sections or two dimensional sheets on twisting become warped into three dimensional sheets.

Saint Venant, in 1853, gave the first correct theoretical solution for non-circular sections.³ Saint Venant's theory states that at any point of an elastic body, the stresses can be readily calculated if the functions representing the components, u , v and w of the displacements are known. He then proposed the Semi Inverse method in which some of the displacements and forces are assumed and the remainder of these quantities are determined so as to satisfy all the equations of elasticity. The method consists of making as many

simplifying assumptions as appear reasonable based on an inspection of the problem, and then showing that the boundary conditions, the equations of equilibrium, and the equations of compatibility are all satisfied.

The concept of Plasticity was first given by Tresca, who stated that a metal yielded plastically when the maximum shear strain attained a critical value.⁴ Saint Venant developed the fundamental equations of plasticity based on some basic assumptions and provided the plastic solution to the torsional problem of a circular shaft.⁵

Much of the work in Plastic torsion is attributed to Nadai, who in 1923, investigated both theoretically and experimentally the plastic zones in a twisted prismatic bar of an arbitrary contour.⁶ From certain properties of the plastic stress function, he came to the conclusion that the plastic stress function is a surface of constant maximum slope over the edge of the cross section under consideration. If a piece of metal is shaped according to the contour of the cross section and covered with sand while lying horizontally, there results a heap of sand. The natural slope of such a heap represents the plastic stress function of the cross section. The natural slope would be a constant slope due to the constancy of the angle of repose of the sand.

Nadai also extended the membrane analogy to determine the stress distribution in a twisted bar after the yield point has been reached.⁷ Let a roof of constant slope be constructed over the contour of the cross section and the base of this roof be closed with a membrane. If the membrane is loaded with pressure, it will bulge upwards, touching some portions of the roof. The touched portion of the membrane represents the plastic regions of the cross section, while the free or untouched portions of the membrane represents elastic regions or the surface of varying shearing stresses.

The stress distributions in a prismatic bar having a solid cross section

and subjected to pure torsion fall under three different classifications:

- (a) Elastic Stress Distribution
- (b) Elastic-Plastic Stress Distribution
- (c) Fully Plastic Stress Distribution

Problems involving elastic stress distributions and fully plastic stress distributions are considered in the following discussion, but elastic-plastic stress distributions are not considered.

2.2 ELASTIC SOLUTIONS TO TORSIONAL PROBLEMS FOR SOLID PRISMATIC MEMBERS

The mathematical analysis of the torsion problem assuming that warping will occur was first performed by Saint Venant, in 1855.³ This analysis leads to the conclusion that the largest shearing stress on a section occurs on the periphery at the point or points nearest to the centroidal axis. In reaching this conclusion, the following two assumptions are fundamental⁸:

- (i) The body forces due to the effect of gravity are neglected.
- (ii) The stress distribution takes place so abruptly that it does not vary with Z (axis of centroid).

If a solid prismatic bar having an arbitrary contour is twisted by couples applied at the ends, then the angle of rotation of a cross section at a distance Z from the origin will be $Z \theta$, where θ is the angle of twist per unit length.

Referring to Figure 1

$$x = p \cos \alpha$$

$$y = p \sin \alpha$$

where p is the radius of circular cross section

$$x = -p \sin \alpha \cdot \delta \alpha$$

$$y = p \cos \alpha \cdot \delta \alpha$$

Let u = displacement in the direction of x -axis.

v = displacement in the direction of y -axis

$$\text{Then } u = \delta x = -y \delta \alpha = -y Z \theta \quad (1)$$

$$v = \delta y = x \delta \alpha = x Z \theta \quad (2)$$

Due to the warping action, the displaced point P' has moved out of the original plane of P by an amount w , where

w = displacement in the direction of z -axis.

Warping is different for different values of x and y but is independent of z so that all cross sections warp in the same manner.

$$w = \theta F(x, y) \quad (3)$$

where F = warping function.

Equation 3 indicates that for a given point, warping is also proportional to θ .

Converting displacements to normal and shearing strains,

$$\epsilon_x = \frac{\partial u}{\partial x} = 0$$

$$\epsilon_y = \frac{\partial v}{\partial y} = 0$$

$$\epsilon_z = \frac{\partial w}{\partial z} = 0$$

$$\gamma_{xy} = \frac{\partial u}{\partial y} + \frac{\partial v}{\partial x} = -z\theta + z\theta = 0$$

$$\gamma_{yz} = \frac{\partial v}{\partial z} + \frac{\partial w}{\partial y} = x\theta + \theta \frac{\partial F}{\partial y}$$

$$\gamma_{xz} = \frac{\partial u}{\partial z} + \frac{\partial w}{\partial x} = -y\theta + \theta \frac{\partial F}{\partial x} \quad (4)$$

Where ϵ are normal strains and γ are shearing strains.

Applying Hooke's law and converting strains to stresses.

$$\sigma_x = \sigma_y = \sigma_z = \tau_{xy} = 0$$

$$\tau_{yz} = G \gamma_{yz} = G(x\theta + \theta \frac{\partial F}{\partial y})$$

$$\tau_{xz} = G \gamma_{xz} = G(-y\theta + \theta \frac{\partial F}{\partial x}) \quad (5)$$

Where σ are the normal stresses and τ are the shearing stresses.

Differentiating and subtracting Eq. 5 to eliminate the warping function,

$$\frac{\partial \tau_{xz}}{\partial y} - \frac{\partial \tau_{yz}}{\partial x} = -2G\theta \quad (6)$$

In the absence of body forces, the only equation of equilibrium not identically satisfied is

$$\frac{\partial \tau_{xz}}{\partial x} + \frac{\partial \tau_{yz}}{\partial y} = 0 \quad (7)$$

Equation 7 is satisfied if the stress components τ_{xz} and τ_{yz} are derived from a stress function $\psi(x, y)$.

$$\begin{aligned} \tau_{xz} &= \frac{\partial \psi}{\partial y} \\ \tau_{yz} &= -\frac{\partial \psi}{\partial x} \end{aligned} \quad (8)$$

Substituting Eq. 8 in Eq. 6,

$$\frac{\partial^2 \psi}{\partial x^2} + \frac{\partial^2 \psi}{\partial y^2} = -2G\theta \quad (9)$$

Which is the required partial differential equation for the stress function. The boundary condition for this equation can be obtained if the parametric equation on contour C are considered as

$$\begin{aligned} x &= x(s) \\ y &= y(s) \end{aligned} \quad (10)$$

Referring to Fig. 2, it is depicted that as x is decreasing, s goes on increasing. This figure represents a triangular element at the boundary of the cross section.

Since there are no normal stresses over the curved surface of the bar,

$$dA \tau_{xz} \sin \theta + dA \tau_{yz} \cos \theta = 0$$

or

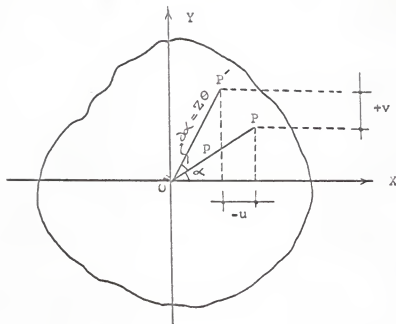


Fig. 1. Twisting of solid prismatic bar having an arbitrary contour.

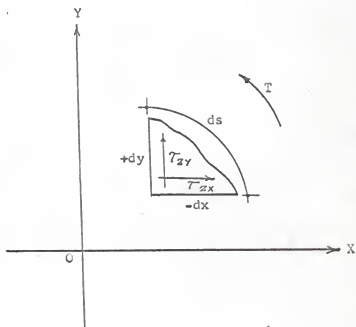


Fig. 2. Boundary condition.

$$\frac{\tau_{yz}}{\tau_{xz}} = \frac{dy/ds}{dx/ds} \quad (11)$$

Substituting Eq. 8 in Eq. 11,

$$-\frac{\partial\psi/\partial x}{\partial\psi/\partial y} = \frac{dy/ds}{dx/ds}$$

or

$$\frac{\partial\psi}{\partial s} = 0$$

$$\text{or } \psi = \text{constant} \quad (12)$$

Since only the first derivative of ψ is useful, it is supposed that $\psi = 0$ on the contour of the cross section.

$$\therefore \psi = 0 \text{ on } C \quad (13)$$

The method of adopting a stress function is least familiar to engineers, and consists in satisfying a differential equation, which follows from the equation of compatibility and the equation of equilibrium. In addition, Hooke's law must be valid throughout.

(a) Circular Cross Sections:

The mathematical treatment for the elastic stresses and deformations induced by torsion is very complicated except in the case of a circular member.

The exact solution of the torsional problem for a circular member is obtained, if it is based on the following two assumptions.⁹

- (i) Cross sections of the member remain plane during twisting.
- (ii) Rotation takes place without any distortion, i.e. no warping action occurs.

The second assumption is valid provided the angle of twist is small.

Consider a shaft fixed at one end and subjected to a couple acting at the other end.

The element is in a state of pure shear. An element abcd, which was

initially rectangular became distorted as shown in Fig. 3.

From Fig. 3 and Fig. 4, the displacement on the transverse side and the longitudinal side should be the same.

$$\therefore L \gamma = P \Theta'$$

$$\text{or} \quad \gamma = P \frac{\Theta'}{L} = P \Theta \quad (14)$$

where L is the length of the member, Θ' is the total angle of twist and Θ is the angle of twist per unit length.

For the same angle of twist,

$$\gamma' = P' \frac{\Theta'}{L} = P' \Theta$$

$$\frac{\gamma}{\gamma'} = \frac{P}{P'} \quad (15)$$

Therefore the shearing strain at any point in the cross section is directly proportional to the distance P from the centroid.

Applying Hooke's law to Eq. 14,

$$\tau = G \gamma = G_P \Theta \quad (16)$$

The above equation shows that maximum shearing stress occurs at points most remote from the centroid. (Refer to Fig. 5).

To determine the relationship between the shearing stresses and the torque, the distributed shearing stresses are equated to the applied torque.⁹

Consider an elemental area, as shown in Fig. 5. The force acting on it will be

$$\begin{aligned} \text{Force} &= \text{Stress} \times \text{area} \\ &= \tau' \times P' d\Theta dP' \end{aligned}$$

$$\text{Moment} = \tau' P'^2 d\Theta dP'$$

Integrating the internal moments and equating them to the externally applied torque,

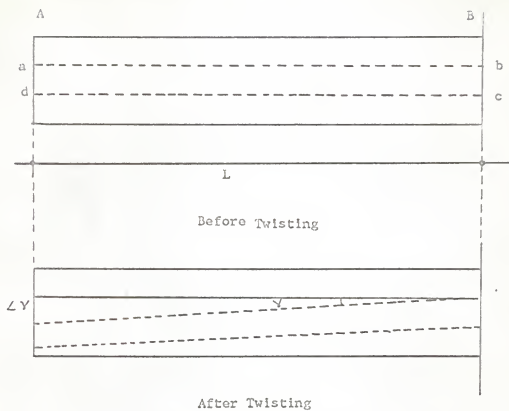


Fig. 3. Distortion on longitudinal side.

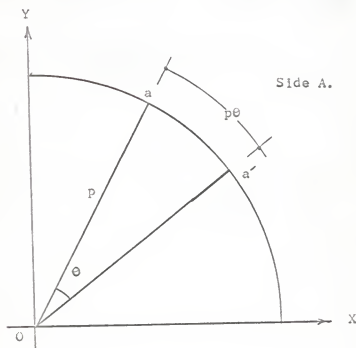


Fig. 4. Distortion on transverse side.

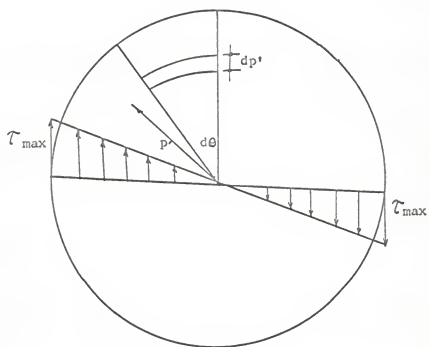


Fig. 5. Stress distribution in circular cross-sections.

$$T = \int_0^P \int_0^{2\pi} \tau' (P')^2 d\theta dP' \quad (17)$$

Substituting the value of T' from Eq. 15 in Eq. 17.

$$\begin{aligned} T &= \int_0^P \frac{2\pi \tau}{P} (P')^3 dP' \\ &= \frac{\tau}{P} \int_0^P (P')^2 (2\pi P' dP') \\ &= \frac{\tau}{P} \int_0^P (P')^2 dA \\ &= \frac{\tau}{P} J \end{aligned} \quad (18)$$

where J is the polar moment of inertia of the cross section

$$\tau = \frac{TP}{J} \quad (19)$$

Equating shear stress to shear strain,

$$\begin{aligned} \gamma &= \frac{TP}{GJ} = P\theta \\ \theta &= \frac{T}{GJ} \end{aligned} \quad (20)$$

Equation 19 is valid only up to the elastic limit. The shearing stress obtained by testing the specimen to rupture and using Eq. 19 is called the shear modulus of rupture.

$$\tau_r = \frac{T_{\max.} P}{J} \quad (21)$$

(b) Rectangular Cross Sections:

In the solution to torsional problems for rectangular cross sections, the membrane analogy has been usefully applied. This was introduced by Prandtl in 1903, and is often referred to as the "Prandtl Analogy".^{10,11}

The stress function can be determined experimentally by means of the analogy, which states that when a homogeneous membrane is supported at the edges of a hole, which has the same outline as that of the cross section of the twisted bar, then the equations representing the shape of the membrane, after being loaded with pressure, are of the same form as those representing the torsional rigidity and stress of a prismatic member having the same cross section as the hole in the plate. The small vertical displacement of the membrane satisfies the differential equation,

$$\frac{\partial^2 z}{\partial x^2} + \frac{\partial^2 z}{\partial y^2} = - \frac{q}{S} \quad (22)$$

where,

q = Intensity of pressure per unit area of membrane.

S = Uniform surface tension per unit length of boundary.

This equation is identical with that of Eq. 9 and it shows that the deflection Z of the membrane will be proportional to the stress function ψ , because ψ and Z are both zero on the contour C . (Refer to Fig. 6 and Fig. 7).

The following informations can be drawn from such a membrane:^{7,12}

- (i) The volume between the membrane and the $Z=0$ plane is proportional to the torque required to cause a twist of Θ per unit length of bar.
- (ii) The inclination of the film surface to the $Z = 0$ plane at any point is simply related to $|\text{grad } \psi|$, the total shear stress at any point.

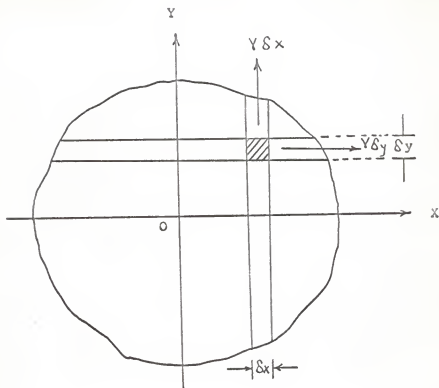


Fig. 6. Membrane in plan.

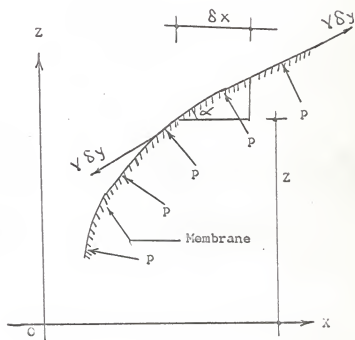


Fig. 7. Membrane in elevation.

- (iii) The location of a series of contour lines show the concentration of stresses at a point; i.e., maximum shear stress occurs at the point where the contour lines are closest to each other.

The solution to torsional problems using the membrane analogy consists in finding a deflection Z , such that it satisfies Eq. 22 and is zero at the boundary.

The condition of symmetry with respect to the y -axis and the boundary condition at the sides $x = \pm a$ of the rectangle are satisfied by taking Z in the form of a series,

$$Z = \sum_{n=1}^{\infty} b_n \left(\cos \frac{n\pi x}{2a} \right) Y_n \quad (23)$$

$$n = 1, 3, 5, \dots$$

where,

b_1, b_3, \dots are constant coefficients

Y_1, Y_3, \dots are functions of y only.

The ultimate solution for maximum shear stress and torque is

$$\tau_{\max} = 2G \Theta A - \frac{16G \Theta a}{\pi^2} \sum_{n=1}^{\infty} \frac{1}{n^2} \left(\frac{1}{n^2 \cos h \frac{n\pi b}{2a}} \right) \quad (24)$$

$$n = 1, 3, 5, \dots$$

$$T = \frac{1}{3} G \Theta (2a)^3 (2b) \left\{ 1 - \frac{192}{\pi^5} \frac{a}{b} \sum_{n=1}^{\infty} \frac{1}{n^5} \tanh \frac{n\pi b}{2a} \right\} \quad (25)$$

$$n = 1, 3, 5, \dots$$

Referring to Fig. 8 it is evident that maximum shear stress occurs at the center of the side nearest to the centroid of the cross section. The variation of stresses on the sides will be parabolic as shown in Fig. 8.

The variation of shear stress along the diagonal has also been determined.

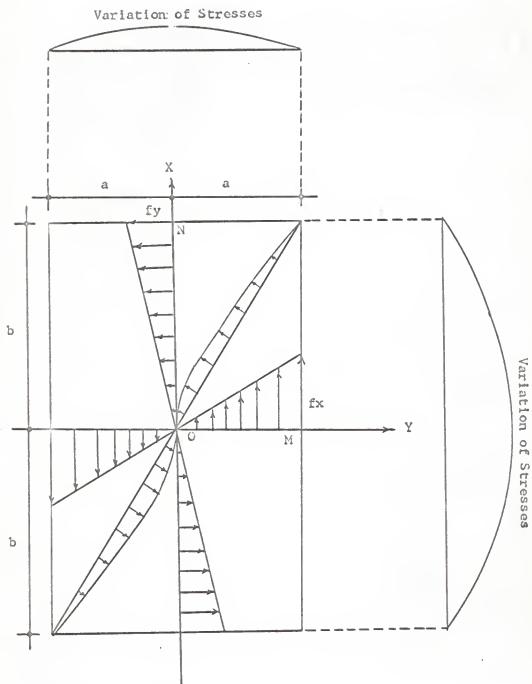


Fig. 8. Stress distribution in rectangular cross-sections.

It is zero at the centroid and at the corners but is maximum at a point nearer to the centroid.

(c) Square Cross Sections

A square cross section is a special case of the rectangular cross section and the formulas for maximum shearing stress and torque can be determined directly from Eq. 24 and Eq. 25 by substituting $a = b$.¹¹

$$\tau_{\max} = 1.351 G a \theta. \quad (26)$$

$$T = 0.1406 G \theta (2a)^4 \quad (27)$$

Referring to Fig. 9, the maximum shearing stress occurs at the centers of the sides, but the shearing stress along the diagonal is zero.

(d) Summary

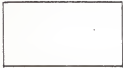
The formulas derived in the preceding sections for pure torsion of solid prismatic members in the elastic range are summarized in Table 1.

2.3 PLASTIC SOLUTIONS TO TORSIONAL PROBLEMS FOR SOLID PRISMATIC MEMBERS

The stress distribution in a prismatic bar subjected to pure torsion can be analyzed in the plastic stage, provided the specimen has a definite plastic limit. This is possible if strain hardening is neglected and an idealized stress - strain diagram is assumed in the form of two straight lines, as shown in Fig. 10.⁶

If the actual stress - strain curve for mild steel is compared with the curve for an elastic, perfectly plastic material (Fig. 10), it is seen that up to point C, where strain hardening starts, mild steel is nearly an elastic, perfectly plastic material. Since most torsional problems deal with mild steel, it would therefore be quite safe to assume an elastic, perfectly plastic material.

Table 1. Elastic solutions to torsion problems for solid prismatic members.

Sections	Equations	Reference Nos.
1 - Circular 	$T_m = \frac{G \cdot \theta \cdot J \cdot L}{L}$ $\tau_{\max} = \frac{G \cdot \theta \cdot P \cdot L}{L}$	11, 12, 13, 14
2 - Rectangular 	$T_m = \frac{1}{3} G \cdot \theta \cdot (2a)^3 (2b) \times$ $\left(1 - \frac{192}{\pi^5} \frac{a}{b} \cdot \sum_{n=1,3,5,\dots}^{\infty} \frac{1}{n^5} \tanh \frac{n\pi b}{2a} \right)$ $\tau_{\max} = 2G\theta a - \frac{16G\theta a}{2} \times$ $\sum_{n=1,3,5,\dots}^{\infty} \frac{1}{n^2 \cosh n \frac{\pi b}{2a}}$	5, 8, 10, 14, 15, 16
3 - Square 	$T_m = 0.1406 G \cdot \theta (2a)^4$ $\tau_{\max} = 1.351 G \cdot \theta \cdot a$	10

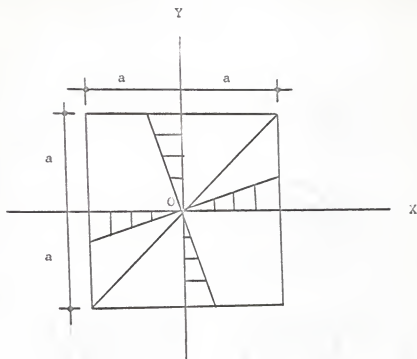


Fig. 9. Stress distribution in Square cross-sections.

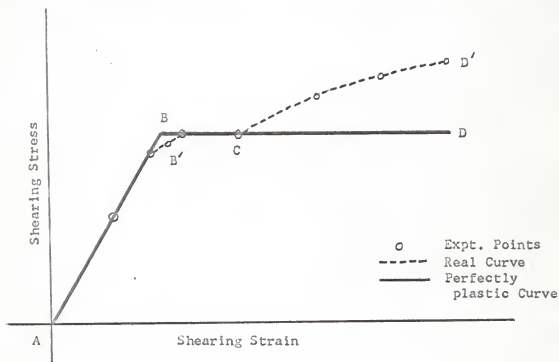


Fig. 10. Idealized Stress-strain diagram for mild steel.

Along curve AB in Fig. 10, the specimen behaves as a perfectly elastic material. As the torque is increased beyond the critical value and the corresponding stress reaches point B, a single or several plastic regions spread into the interior of the cross section, starting from the point or points where the yield stress was first reached. (Refer to Fig. 11) Although practically it is impossible to obtain a perfectly plastic material as shown in Fig. 11, theoretically it is assumed that the cross section is wholly plastic.

For a fully plastic member, the shear stress (Refer to Eq. 8) must be a constant k' .

$$\tau_x^2 + \tau_y^2 = k^2 \quad (28)$$

The equilibrium condition

$$\frac{\partial \tau_{xz}}{\partial x} + \frac{\partial \tau_{yz}}{\partial y} = 0 \quad (29)$$

is still valid in the plastic case.

If $\psi(x, y)$ is the plastic stress function of the cross section, then

$$\begin{aligned} \tau_{xz} &= \frac{\partial \psi}{\partial y} \\ \tau_{yz} &= -\frac{\partial \psi}{\partial x} \end{aligned} \quad (30)$$

These are similar to Eq. 8 of the section on elastic stress.

Substituting Eq. 30 in Eq. 20,

$$\left(\frac{\partial \psi}{\partial x}\right)^2 + \left(\frac{\partial \psi}{\partial y}\right)^2 = k^2 \quad (31)$$

Expressing the above constant in terms of the plastic stress function,

$$|\text{grad } \psi| = k \quad (32)$$

From the above mentioned properties of ψ , it is evident that the plastic stress function is a surface of constant maximum slope constructed over the edge of the cross section.

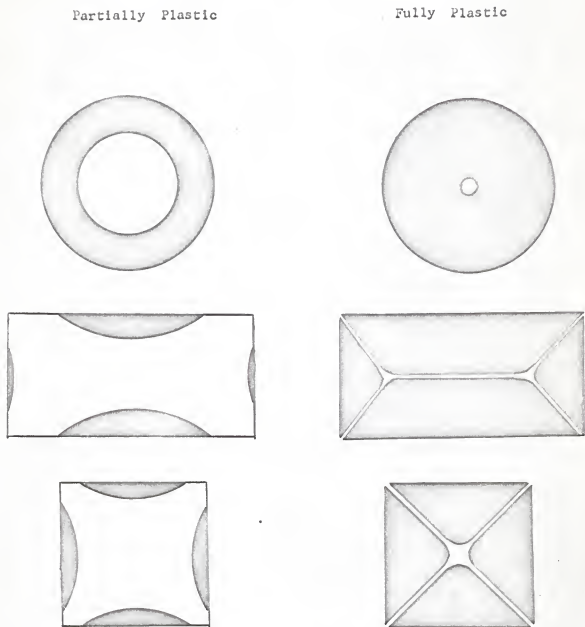


Fig. 11. Development of plastic regions.

The Soap film - Sand hill analogy was derived by Nadai and consists of obtaining the stress function experimentally.⁶

If a horizontal base having the shape of the cross section of the specimen is cut out and covered with sand, then there results a heap, whose natural slope is the same as the surface of stress function ψ . From this heap of sand, a transparent roof under constant slope may be constructed over the edges of the cross section under consideration (Refer to Fig. 12). The plane base of the roof is covered with a membrane, which is then subjected to pressure. For small pressures, the membrane will not touch the roof and it indicates that the cross section is perfectly elastic. As the pressure is increased, a stage is reached when a portion of the membrane touches the roof. The constrained portion of the membrane will satisfy all the conditions of the plastic stress function while the free membrane will satisfy the conditions for the elastic stress function. When the pressure is increased to such an extent that the whole membrane is in contact with the roof (a condition difficult to obtain, refer to Fig. 11), then the cross section is completely plastic.

The shearing stress is equal to the slope of the stress surface and the values of the twisting moment approach a value given by twice the space occupied by the plastic stress surface.

(a) Circular Cross Sections

The stress function for a solid circular member of radius P is,¹³

$$\psi = k(p - R) \quad (33)$$

and the maximum plastic torque T_0 for a solid prismatic section is given by,

$$T_0 = 2 \int_A \psi \, dA$$

where A = area.

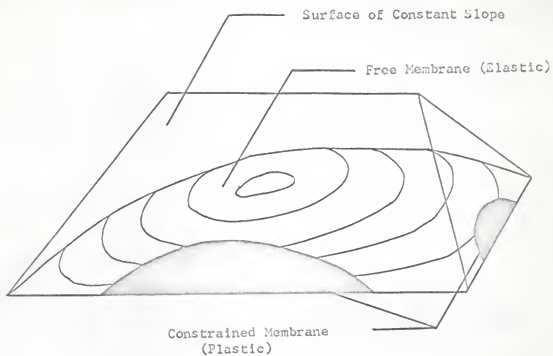


Fig. 12. Soap film-Sand heap analogy.

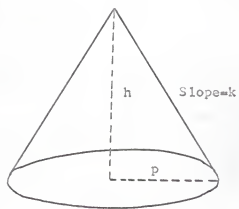


Fig. 13. Sand heap for circular cross-sections.

For a circular cross section,

$$\begin{aligned}
 A &= \pi R^2 \\
 \frac{dA}{dR} &= 2\pi R \\
 T_o &= 2 \int_0^P K(p-R) 2\pi R dR \\
 &= 4\pi K \left\{ p \frac{R^2}{2} - \frac{R^3}{3} \right\} \\
 &= 4\pi K \left\{ \frac{p^3}{2} - \frac{p^3}{3} \right\} \\
 &= \frac{2}{3} \pi K p^3
 \end{aligned} \tag{34}$$

where

$$\begin{aligned}
 K &= \frac{\sigma_0}{2} \text{ (for Tresca's Theory)} \\
 &= \frac{\sigma_0}{\sqrt{3}} \text{ (for Von Mises Theory)}
 \end{aligned}$$

The same problem can be solved by the sand-heap analogy.⁶ The roof of constant slope will be represented by a cone. (Refer to Fig. 13)

$$\text{Slope of heap} = K$$

$$\text{then } h = Kp$$

$$V = \frac{1}{3} \pi p^2 h$$

$$= \frac{1}{3} \pi p^3 k$$

$$T_o = 2V = \frac{2\pi}{3} k p^3$$

(b) Rectangular Cross Section

The rectangular cross section can be solved very easily by the sand-heap analogy.⁶ The resulting heap for such a cross section would be as

shown in Fig 14 (a) and Fig. 14 (b).

Constant slope = Ka

$$\text{Vol. 1} = 2 \times \frac{1}{3} \times 2a \times a \times Ka$$

$$= \frac{4}{3} Ka^3$$

$$\text{Vol. 2} = \frac{1}{2} \times 2(b-a) \times 2a \times Ka$$

$$= 2 Ka^2 (b-a)$$

$$V = \frac{4}{3} Ka^3 + 2Ka^2 (b-a)$$

$$T_o = 2V = \frac{8}{3} Ka^3 + 4Ka^2 (b-a) \quad (35)$$

(c) Square Cross Section

For a square cross section with sides of $2a$, the stress function is,¹³

$$\psi = K(a-x)$$

Now $A = 4x^2$

$$\frac{dA}{dx} = 8x$$

$$T_o = 2 \int_a^A \psi dA$$

$$= 2 \int_0^a K(a-x) 8x dx$$

$$= 16 K \left\{ a \frac{x^2}{2} - \frac{x^3}{3} \right\}_0^a$$

$$= 16 K \left\{ \frac{a^3}{2} - \frac{a^3}{3} \right\}$$

$$= \frac{8}{3} Ka^3 \quad (36)$$

The same results will be obtained if the sand-heap analogy is applied.

Referring to Fig. 15 (a) and Fig. 15 (b)

Let slope of heap = K

The height h = Ka

$$V = \frac{1}{2} \times 2a \times 2a \times ka$$

$$= \frac{1}{2} Ka^3$$

$$T_o = 2V = \frac{8}{5} Ka^3$$

(d) Summary

The formulas for plastic torsion of solid prismatic members which are derived in the preceding sections are summarized in Table 2.

3 EXPERIMENTAL PROGRAM

3.1 GENERAL

The foregoing discussion will be based on the methods and procedures adopted to determine the required torsional properties of the specimens. Since the torsional properties of a particular material are dependent upon its yield strength, it was necessary to conduct tensile tests first before starting the torsion investigation.

3.2 DESIGN OF TENSILE TEST EXPERIMENTS

(a) Test Specimens

The tensile test specimens were prepared from the mild steel torsion bars conforming to the requirements of AISI C - 1020.

Tensile tests were conducted on eleven different specimens. These specimens were fabricated from the same material used for the torsion test specimens, one tensile test specimen often serving for more than one torsion test bar.

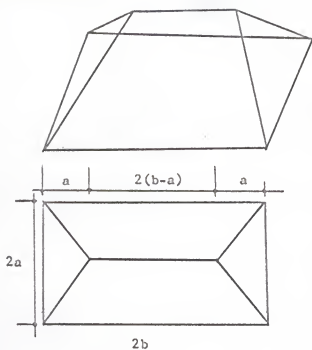


Fig. 14. Sand heap for rectangular cross-sections.

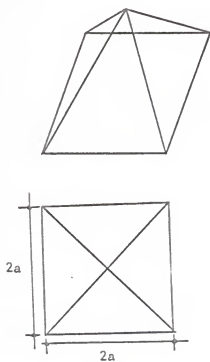
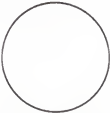
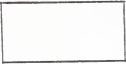
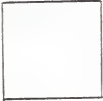


Fig. 15. Sand heap for square cross-sections.

Table 2. Plastic solutions to torsion problems for solid prismatic members.

Sections	Equations	Reference Nos.
1 - Circular	$T_0 = \frac{2\pi}{3} \frac{\sigma_0}{\alpha} \cdot p^3$	6, 7, 17
		
2 - Rectangular	$T_0 = \frac{8}{3} \frac{\sigma_0}{\alpha} a^3 +$	6, 7
2a	$4 \frac{\sigma_0}{\alpha} a^2 (b - a)$	
		
2b		
3 - Square	$T_0 = \frac{8}{3} \frac{\sigma_0}{\alpha} a^3$	17
2a		
		
2a		

(Refer to Fig. 17) The eleven tensile specimens included four rectangular specimens, two circular specimens with non-threaded ends and four circular specimens with threaded ends.

The dimensions of all the tensile test specimens are shown on Figs. 19 and 20.

(b) Apparatus Used

The apparatus used for the tensile tests was a 20,000 lb capacity Riehle Universal Screw-Type machine, which had five different load ranges, e.g. 1,000 lb, 2,000 lb, 5,000 lb, 10,000 lb and 20,000 lb. Elongations were obtained with a 2" extensometer for the first (elastic) portion of each test; while machinist's dividers were used after the elongations exceeded the maximum stroke of the extensometer.

(c) Experimental Procedure

The tensile test specimens were punched for a 2" gage length and then gripped in the machine fixtures. After the load indicating dial had been zeroed and the initial gage length recorded by means of the dividers, the extensometer was attached to the specimen. The load was then applied at a cross head speed of approximately 0.01 in/min. and a continuous curve of Load vs Elongation was obtained on a recorder. The strain rate for 1 inch of graph on the recorder was 0.004 in/2in.

The load-elongation curve (see Fig. 21) was plotted by the recorder until the extensometer was reached, at which point the loading was held constant, the extensometer removed and the elongation checked with the dividers. The loading was then resumed and the elongation recorded by means of the dividers at certain convenient intervals of time. This process was continued until the specimen fractured.

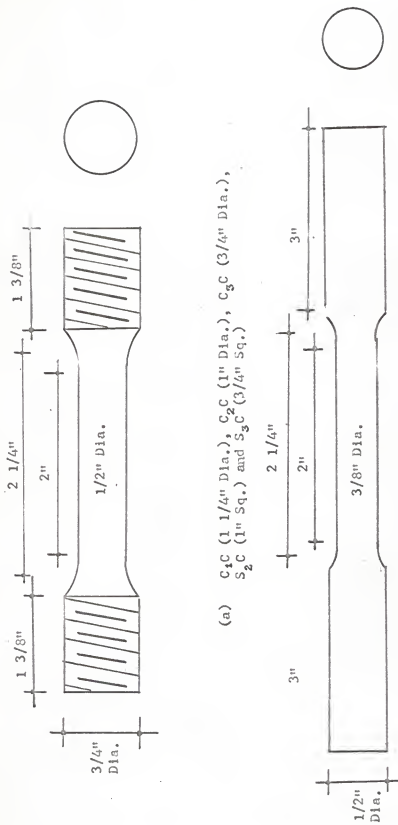
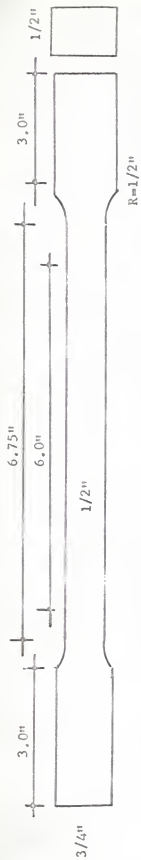
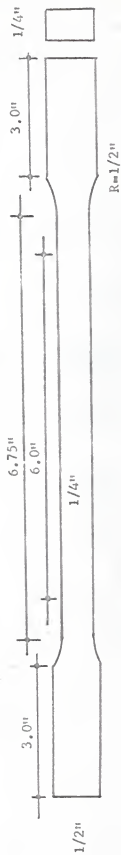


Fig. 19. Tensile test coupons (Circular and Square).



(a) R_2^C (1" 1/2" Flat) and R_3^C (3/4" 1/2" Flat)



(b) R_3^C (3/4" 1/4") and R_4^C (1/2" 1/4")

Fig. 20. Tensile test coupons (Rectangular).

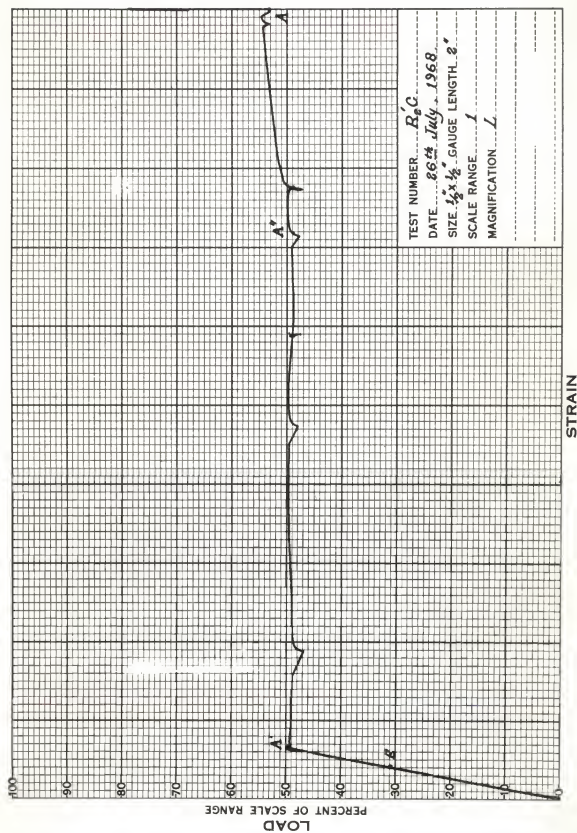


Figure 21. Load-Strain Curve.

In two cases, namely, specimens R_{2c}^1 and R_{3c} , Poisson's ratio was also determined. This was accomplished by using strain gages oriented perpendicular to the longitudinal axis of the specimen. The transverse strain was recorded by means of a strain indicator. The readings for the transverse strain were taken at 1,000 lb load increments. After the proportional limit, these readings were discontinued.

3.3 DESIGN OF TORSION TEST EXPERIMENTS

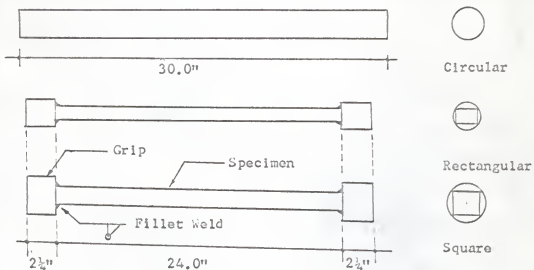
(a) Test Specimens

The specification for the torsion test specimen material was the same as that of the tensile test specimens described earlier.

The basic problem for the torsion test specimens was to obtain them from the practical sizes available from the dealers or manufacturers. For circular and square cross sections, this presented no problem; however, rectangular cross sections were available only in sizes of $1" \times \frac{1}{2}"$, $\frac{3}{4}" \times \frac{1}{2}"$, $\frac{3}{4}" \times \frac{1}{4}"$ and $\frac{1}{2}" \times \frac{1}{4}"$. Certain cross sections were therefore machined from the above mentioned sizes. (Refer to Fig. 20) Several different cross section sizes were chosen for each shape, as summarized in Table 3.

The maximum clear distance between the ends of the two grips in the testing machine was 28". However, for all tests in this investigation the effective length of specimen was 24". The grip length at each end of the specimen was $2\frac{1}{4}"$.

The rectangular and square test specimens were welded to circular grips. The thicknesses of the fillet-welds between these grips and the specimens are shown in Table 3.



S.No.	Specimen Number	Bead of Fillet Weld
1.	R ₂	1/4"
2.	R ₃	1/4"
3.	R ₄	3/16"
4.	R' ₂	3/16"
5.	R' ₃	3/16"
6.	R' ₄	1/8"
7.	R'' ₂	3/16"
8.	R'' ₃	3/16"
9.	R'' ₄	1/8"
10.	S ₂	3/8"
11.	S ₃	1/4"
12.	S ₄	1/4"

Table 3. Dimension of welds.

(b) Apparatus Used

The testing apparatus consisted of a Tinius Ohlsen gear type torsion testing machine, the capacity of which is 10,000 in. lbs. (Refer to Fig. 22) This machine consists of a torque wheel, which is rigidly fastened to the main shaft. There are housings in the machine which prevent the development of bending moment. Triangular chucks in the machine hold the specimens firmly at the ends. These chucks accommodate circular cross sections with a maximum diameter of 1.5 inch. The readings of the applied torque and angle of twist can be measured directly on the machine. The machine could be operated manually as well as electrically.

Preliminary experiments were carried out to check the operation of the machine. The results of these tests indicated the possibility of erroneous readings from the twist gage on the machine. It was also determined in these tests that the twist gage on the machine did not take into account the slip in the grips. For these reasons, another twist measuring device was designed and constructed. This device consisted of two circular steel rings each having an internal diameter of $1\frac{3}{4}$ " and a length of $\frac{1}{4}$ ". One steel ring was attached to a pointer and the other attached to a circular plate, 22 in. in diameter and $\frac{1}{4}$ " thick, by means of screws. At the periphery of the plate, angles were marked in degrees. The steel rings were each provided with four Alan screws to fix them firmly to the specimen. The twist measuring device is shown in Fig. 23.

Strains were measured experimentally for specimens S_2 , R_2 , R_2' and R_2'' . Electrical resistance Strain Rosettes were used for this purpose and the strain readings obtained with a strain indicator. (Refer to Fig. 23)



Fig. 22 Tinius Ohlsen torsion testing machine.

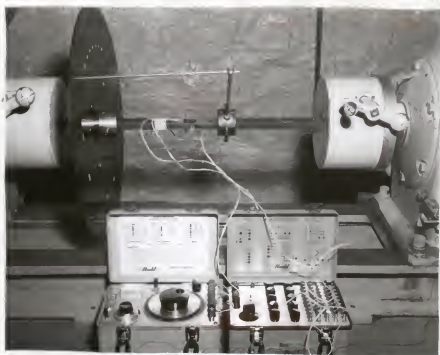


Fig. 23 Strain gage connections for torsion test specimens.

(c) Experimental Procedure

After the specimens had been fabricated, the exact dimensions of each cross section were measured at intervals of $\frac{3}{8}$ " by means of a micrometer. These dimensions are shown in Fig. 16, 17 and 18. The average dimensions were then calculated and are tabulated in Table 4.

The grips of the specimen were cleaned with wire brushes and one end was fixed in the chucks of the machine. The twist measuring device was then adjusted on the specimen so as to measure the angle of twist over a gage length of 10". The torque dial and twist dial were both zeroed before the test was started.

In the early stages of the torque-twist curve (i.e. in the elastic range), the torque increases very rapidly for a small change in the angle of twist. It was therefore necessary to apply the torque manually during the first complete rotation of the specimen. In the elastic range, the torque was applied to a value of one third the anticipated yield torque, and then subsequently released. This cycle was repeated three or four times so that slippage in the grips could be eliminated. The exact initial torque and angle of twist were taken after these cycles had been completed. The torque was increased very slowly and readings were recorded every half degree of twist. This process was continued manually for one complete rotation, after which the torque was applied with the electric motor. Readings were then taken after each 100° of revolution measured by the machine twist gage.

When the specimen failed, the location of failure was carefully observed and checked to see that failure did not occur in the welds or the heat affected zones of the welds.

As previously mentioned, strain rosettes were used on some of the specimens, to measure strains. The three gages of a strain rosette were connected to three

Table 4. Dimensions of specimens to be tested.

Sections	Designation	Proposed Cross- Sectional Dimensions	Measured Cross- Sectional Dimensions
1-Circular	C ₁	2p = 1.250	2p = 1.256
	C ₂	2p = 1.000	2p = 0.991
	C ₃	2p = 0.750	2p = 0.750
	C ₄	2p = 0.500	2p = 0.497
2-Rectangular	R ₂	2b = 1.000	2b = 1.003
		2a = 0.666	2a = 0.659
	R ₃	2b = 0.750	2b = 0.762
		2a = 0.500	2a = 0.501
	R ₄	2b = 0.500	2b = 0.499
		2a = 0.333	2a = 0.341
	R ₂ '	2b = 1.000	2b = 1.009
		2a = 0.500	2a = 0.501
	R ₃ '	2b = 0.750	2b = 0.756
		2a = 0.375	2a = 0.375
	R ₄ '	2b = 0.500	2b = 0.516
		2a = 0.250	2a = 0.250
	R ₂ ''	2b = 1.000	2b = 1.008
		2a = 0.333	2a = 0.336
R ₃ ''	2b = 0.750	2b = 0.760	
	2a = 0.250	2a = 0.252	
R ₄ ''	2b = 0.500	2b = 0.500	
	2a = 0.166	2a = 0.160	
3-Square	S ₂	2a = 1.000	2a = 1.002
	S ₃	2a = 7.50	2a = 0.765
	S ₄	2a = 0.500	2a = 0.504

channels of a switch box and readings were taken with a strain indicator at convenient intervals of torque.

In order to obtain accurate strain gage readings, a specimen was first loaded to three fourths the value of the anticipated yield torque and then unloaded. It was again loaded, unloaded and again loaded. During this process of loading and unloading, strain readings were taken and checked with each other. After the yield torque had been reached strain readings were not taken because Hooke's Law does not apply in the inelastic range, and therefore Mohr's circle for stress and strain is not valid.

It should be mentioned that the testing machine could not be operated beyond 8,600 lb in. although the nominal capacity is 10,000 lb in. Therefore, four specimens (C_1 , C_2 , S_2 and R_2) could not be tested to failure.

4 PRESENTATION AND INTERPRETATION OF DATA

4.1 MATERIAL PROPERTIES FROM TENSION TESTS

The material properties were determined from tensile tests, as explained in chapter 3. The required material properties included the yield stress, the ultimate tensile stress, the modulus of elasticity, Poisson's Ratio and the percent elongation. A typical load-elongation curve is shown in Fig. 21. This curve was recorded directly from the extensometer during the test on specimen R_2C .

A stress-strain curve was obtained from the load-elongation curve of the recorder and from the subsequent elongation readings taken by the machinist's divider. In Fig. 24, the stress-strain curve up to point A was drawn from the recorder plot and from A to R_1 , the curve was obtained from the divider elongation readings.

Some of the divider points, i.e. B, D, E, etc., have not been shown on the

stress-strain curve in Fig. 24 because of the small scale adopted for strain in this figure.

The initial stress-strain curve is linear. On further straining, the relation between stress and strain is no longer linear and the material undergoes plastic deformation. The plastic deformation continues until point A, after which the stress starts increasing with further strain. This effect of the material being able to withstand a greater load despite the reduction in cross sectional area is known as strain hardening. At point G, the rate of strain hardening is unable to keep pace with the rate of reduction in the cross sectional area and a maximum value of the stress is attained, followed by necking of the bar and leading to fracture at R₁.

The yield stress and the ultimate tensile stress of specimen R₂C were found to be 39,200 psi and 63,800 psi, respectively. (Refer also to Table 5)

The modulus of elasticity was obtained from the slope of the elastic portion of the stress strain curve and found to be 31.0×10^6 psi for this specimen.

The percent elongation is calculated by subtracting the initial strain reading from the final strain reading and dividing the result by the original gage length of the specimen.

Final strain reading	= 2 103/128"
Initial strain reading	= 2"
Difference	= 103/128"
Percent elongation	= $103/128 \times \frac{1}{2} \times 100$
	= 40.2%

Poisson's Ratio is obtained by dividing the transverse strain obtained from the strain gage readings by the longitudinal strain.

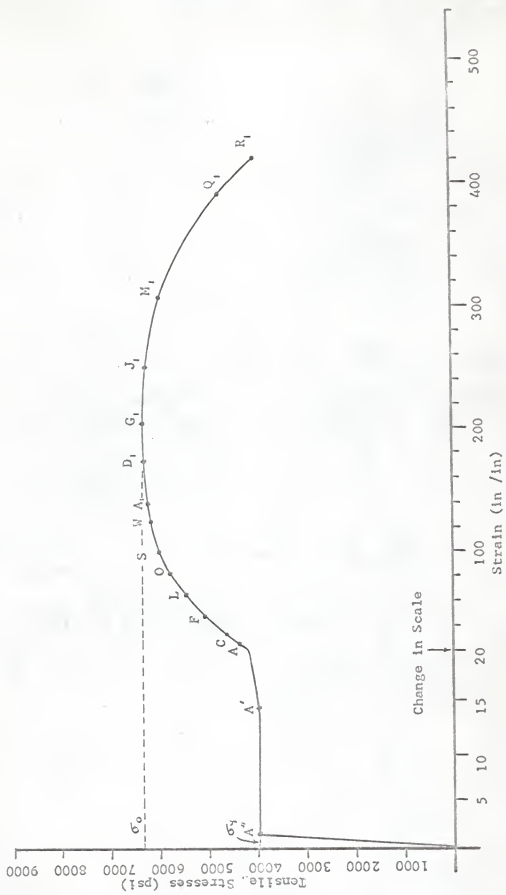


Fig. 24. Tensile stress-strain curve for specimen K₂.

Table 5.

Specimen No.	Yield Strength (psi)	Ultimate Strength (psi)	Modulus of Elasticity (psi)	Percentage Elongation (%)	Poisson's Ratio
C ₁ C	36,900	61,600	32.0 x 10 ⁶	42.0	*
C ₂ C	38,400	62,300	33.3 x 10 ⁶	40.6	*
C ₃ C	38,600	63,700	30.5 x 10 ⁶	38.3	*
C ₄ C	43,000	63,500	29.0 x 10 ⁶	36.0	*
R ₂ 'C } R ₂ ''C }	39,200	63,800	31.0 x 10 ⁶	42.0	0.281
R ₃ 'C } R ₃ ''C } R ₄ 'C }	50,800	69,160	30.8 x 10 ⁶	37.5	0.301
R ₃ ''C	40,400	60,080	29.0 x 10 ⁶	25.4	*
R ₄ 'C } R ₄ ''C }	45,900	61,950	29.0 x 10 ⁶	32.0	*
S ₂ 'C } R ₂ 'C }	38,800	63,000	33.1 x 10 ⁶	41.8	*
S ₃ C	45,220	67,400	29.3 x 10 ⁶	40.6	*
S ₄ C	43,750	68,000	29.8 x 10 ⁶	37.5	*

*Properties not determined.

Final transverse strain	= 1174×10^{-6}
Initial transverse strain	= 842×10^{-6}
Difference	= 332×10^{-6}
Total longitudinal strain	= $\frac{0.004}{2} \times 0.59$
Poisson's Ratio	= $\frac{332 \times 10^{-6}}{\frac{0.004}{2} \times 0.59}$
	= 0.282

Similar calculations were made for all the specimens and the resulting values have been summarized in Table 5.

4.2 TORQUE-TWIST CURVES

The torque-twist curves for all the specimens are shown in Figs. 25 through 32.

It would not be worthwhile to discuss the torsional behaviour of all the specimens separately; instead, the torque-twist curve for a sample specimen (R_2') will be discussed in detail and the determination of the torsional properties described.

The data for specimen R_2' is presented in Table 6. A complete torque-twist curve for this specimen is shown in Fig. 35. (The torque-twist curves in Figs. 25 to 32 have not been shown up to the point of failure; instead, they indicate only the elastic and plastic torque.) Referring back to the torque-twist curve of specimen $R_2'C$ in Fig. 35, the initial part of the curve is perfectly elastic. This is shown in the form of a straight line OB. At B, the stress at the center of the longest side of specimen R_2' reached the yield point. The yielded zone expanded with increasing torque until, theoretically, the whole cross section became plastic. It is not possible to determine the part of the curve for which the specimen remained elastic-plastic. The reason

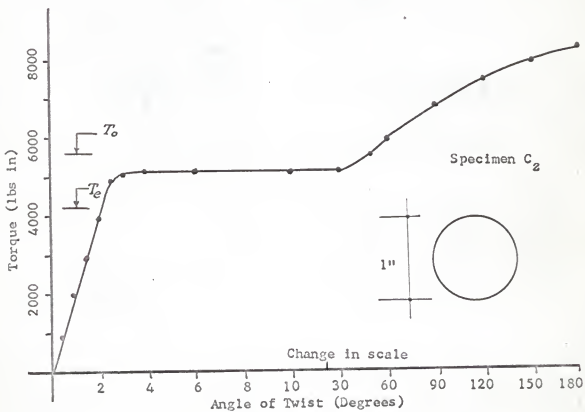
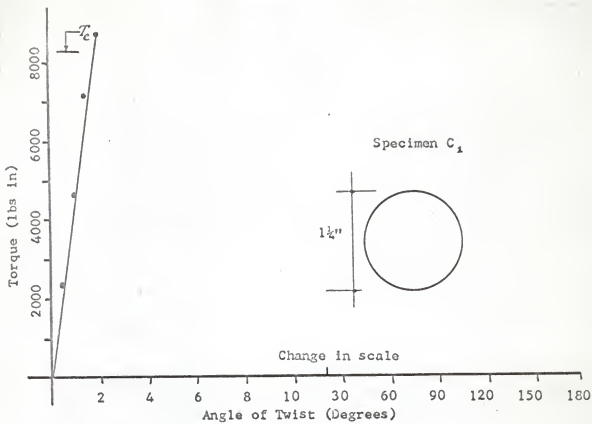


Fig. 25. Torque-twist curve.

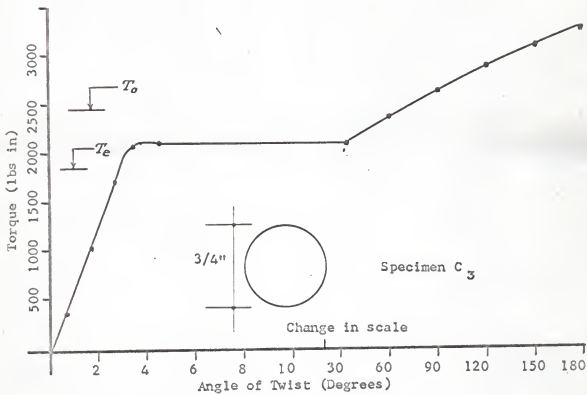
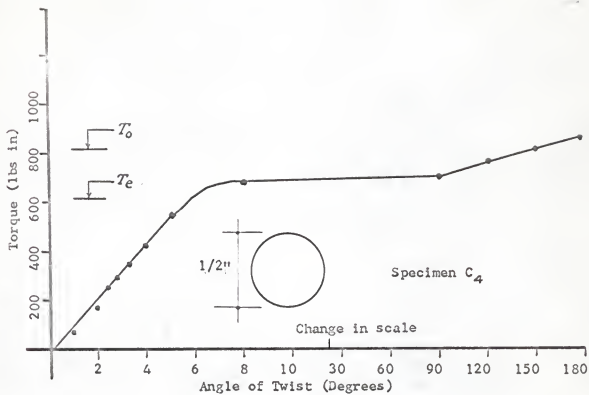


Fig. 26. Torque-twist curve.

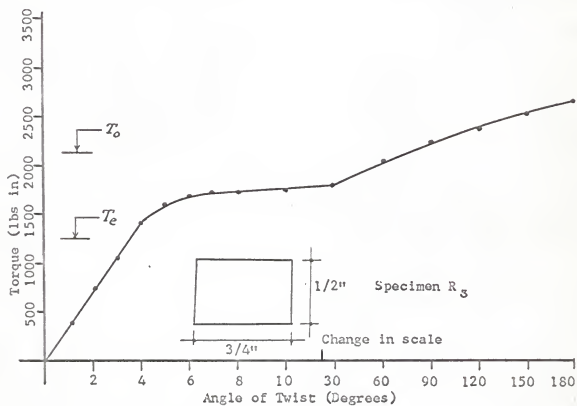
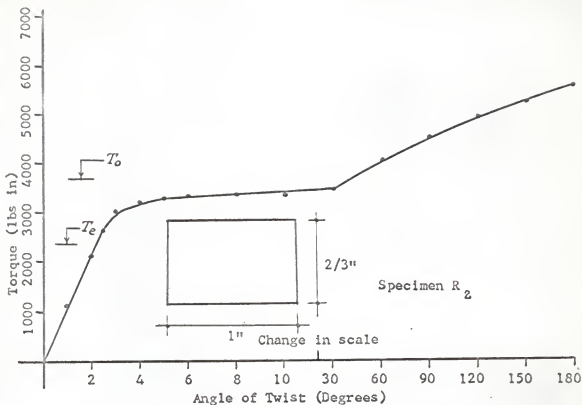


Fig. 27. Torque-twist curve.

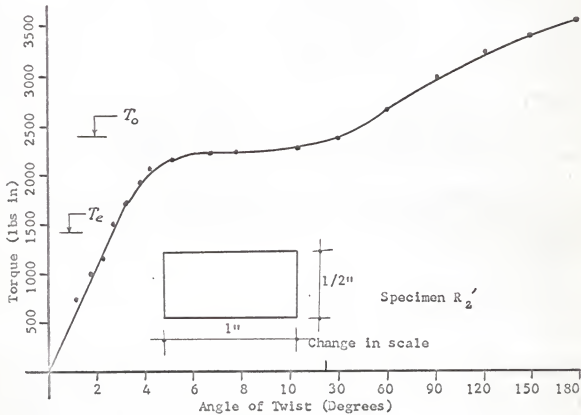
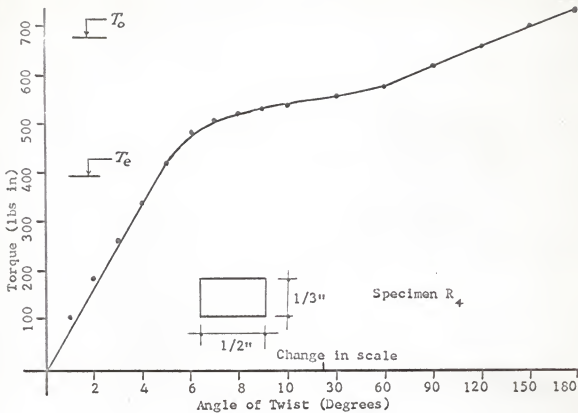


Fig. 28. Torque-twist curve.

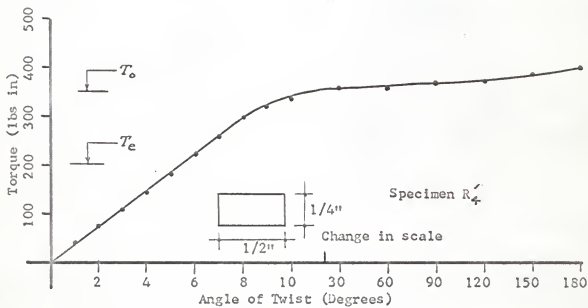
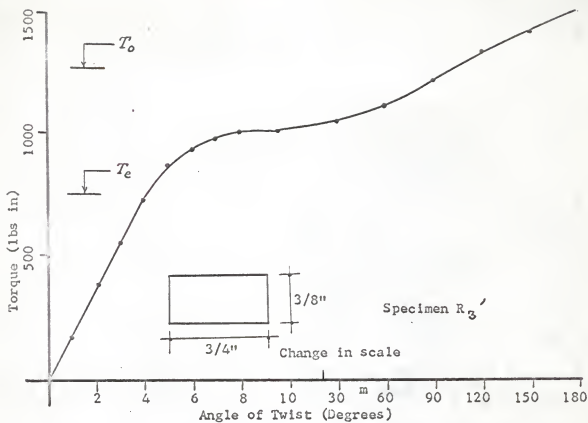


Fig. 29. Torque-twist curve.

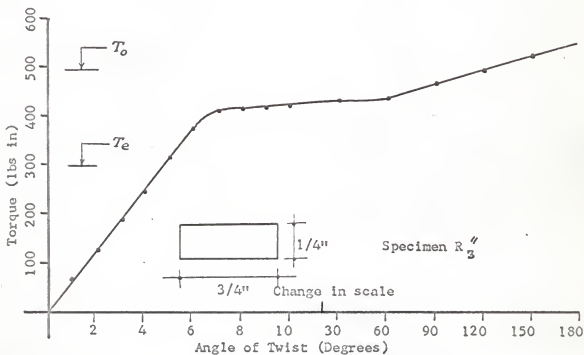
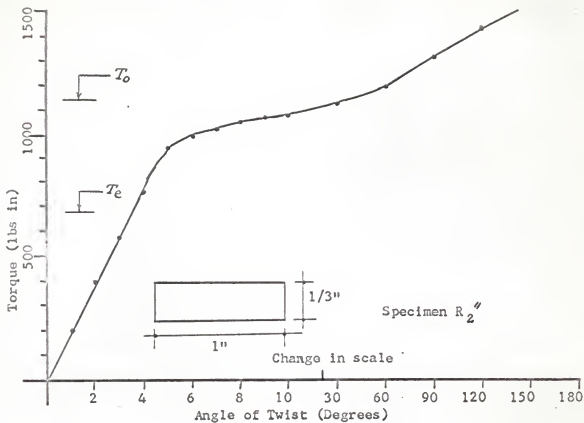


Fig. 30. Torque-twist curve.

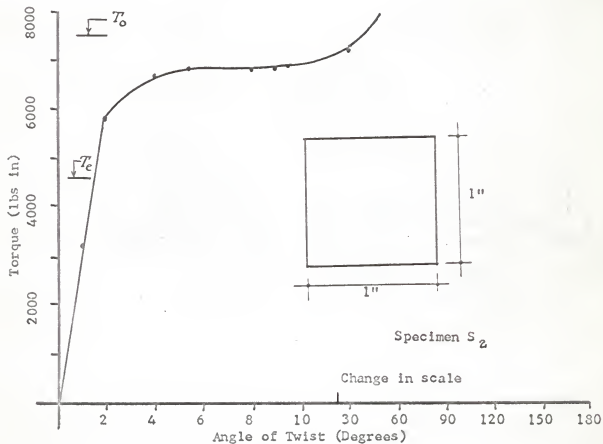
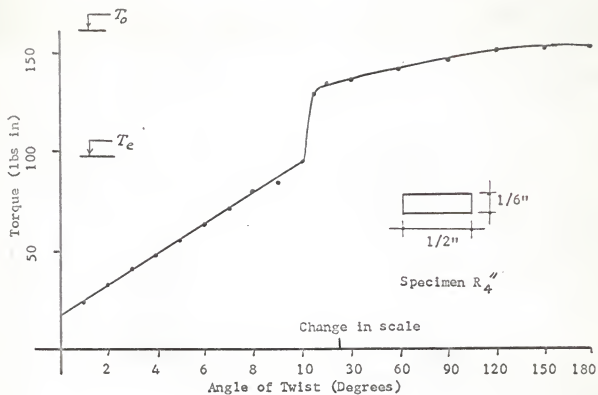


Fig. 31. Torque-twist curve.

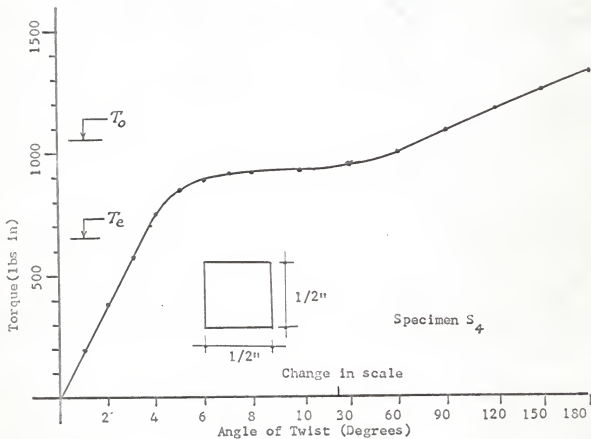
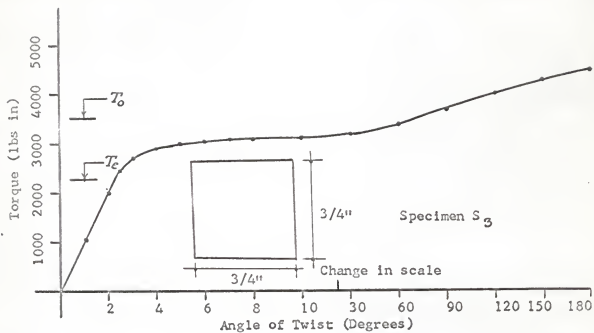


Fig. 32. Torque-twist curve.

Table 6.

Specimen No. : R₂¹
 Crosssectional Dimensions . . . : 1" X $\frac{1}{2}$ "
 Total Eff. Length : 23 $\frac{3}{4}$ "
 Eff. Length For Twist Gage. . . : 10"
 Yield Strength. : 39,200 psi

Total Ang. of Twist (Deg.)	Angle from Twist gage (Deg.)	Torque (lb.in.)	ϵ_1	ϵ_2	ϵ_3
$2\frac{3}{4}$	$-2\frac{3}{4}$	0	2680	3106	200
$3\frac{3}{4}$	$-2\frac{1}{2}$	250	2680	2975	330
5	-2	500	2680	2831	468
6	$-1\frac{1}{2}$	750	2671	2687	608
$7\frac{1}{2}$	-1	1000	2664	2542	749
9	$-\frac{1}{2}$	1250	2656	2400	890
$10\frac{1}{2}$	0	1500	2650	2252	1032
Unloading					
$9\frac{1}{4}$	$-\frac{1}{2}$	1250	2650	2395	895
8	-1	1000	2652	2541	750
7	$-1\frac{1}{2}$	750	2652	2680	614
6	-2	500	2654	2827	473
5	$-2\frac{1}{2}$	250	2654	2973	331
$3\frac{3}{4}$	$-2\frac{3}{4}$	0	2654	3110	200
Loading					
5	$-2\frac{1}{2}$	250	2652	2971	332
6	-2	500	2652	2830	473
		750	2651	2680	618

Table 6. (Contd.)

Total Ang. of Twist (Deg.)	Angle from Twist gage (Deg.)	Torque (lb.in.)	ϵ_1	ϵ_2	ϵ_3
8	-1	1000	2651	2535	756
		1250	2650	2391	900
$10\frac{1}{2}$	0	1500	2650	2250	1036
		Unloading.			
		1250	2650	2392	896
8	-1	1000	2651	2540	753
		750	2651	2682	613
		500	2653	2826	475
		250	2653	2972	331
		0	2653	3110	200
		Loading			
+4	$-\frac{3}{4}$	0	2653	3110	200
5	$-2\frac{1}{4}$	250	2653	2970	335
6	-2	500	2653	2825	476
7	$-1\frac{1}{2}$	750	2650	2675	620
8	-1	1000	2650	2535	755
$9\frac{1}{4}$	$-\frac{1}{2}$	1250	2650	2390	900
$10\frac{1}{2}$	0	1500 A	2648	2250	1038
12	$\frac{1}{2}$	1720	2645	2127	1156
$13\frac{1}{2}$	1	1930	2625	1850	1370
15	$1\frac{1}{2}$	2045 B	2621	1553	1697
16	2	2100	2618	1260	1928
17	$2\frac{1}{2}$	2150	2614	1010	2161

Table 6. (Contd.)

Total Ang. of Twist (Deg.)	Angle from Twist gage (Deg.)	Torque (lb.in.)	ϵ_1	ϵ_2	ϵ_3
18	3	2160	2613	732	2400
$19\frac{3}{4}$	4	2210	2613	205	2910
$21\frac{1}{2}$	5	2240	2607	0	3420
28	9	2280			
$29\frac{1}{2}$	10	2280 C			
$36\frac{3}{4}$	15	2300			
44	20	2300			
$53\frac{1}{2}$	25	2330			
$65\frac{1}{2}$	30	2370 D			
95	40	2460 E			
$121\frac{1}{2}$	50	2580 F			
144	60	2690			
168	70	2800			
190	80	2900 G			
213	90	3000 H			
283	120	3230 I			
350	150	3420 J			
58	180	3600 K			
122	210	3750 L			
190	240	3900 M			
255	270	4030 N			
322	300	4160 O			
30	330	4280 P			

Table 6. (Contd.)

Total Ang. of Twist (Deg.)	Angle from Twist gage (Deg.)	Torque (lb.in.)	ϵ_1	ϵ_2	ϵ_3
97	0	4390 Q			
180	36	4520 R			
0	115	4790 S			
180	197	5050 T			
0	275	5280 U			
180	355	5550 V			
0	74	5790 W			
180	150	6000 X			
0	229	6180			
90	244	6240			

(Fracture)

Fracture occurred at the left hand grip.

for this is that strain hardening started in some portions of the plastic zone and the slope of the curve increased. Point C on the curve indicates that most of the cross section of specimen R_2' has become plastic. The effect of strain hardening increased (i.e. slope of curve increases) as more torque was applied until fracture occurred at D. (The fractured torsion specimens are shown in Fig. 38 to 42.)

The shear modulus of elasticity (G) can be determined from the slope of the elastic portion of torque-twist curve, and this value for R_2' was found to be 10.95×10^6 psi. The values of the shear modulus for the other specimens are given in Table 7.

A comparison of the torque-twist curves is shown in Figs. 33 to 37. It is evident from these curves that the circular bars can sustain a larger total angle of twist than the non-circular ones. This behaviour of the circular bars is justified on the basis of complete symmetry about the longitudinal axis. According to the assumption that plane cross sections remain plane during twisting, the shearing strains are uniform on any circular ring and are not accompanied by any displacement normal to the cross section.

However, for the non-circular specimens, the shearing strains are not uniform around the periphery. The only way varying strains of this type can be accommodated is by warping of each cross section out of its original plane. The total displacement is then the rotational displacement added to the displacement normal to the plane of the cross section. The non-circular bars therefore fail at a smaller total angle of twist than the circular ones for the same effective length.

The transition in the torque-twist curves from the elastic range to the plastic range, in the case of the non-circular specimens, is gradual, whereas in the case of the circular specimens, this transition is quite abrupt. This

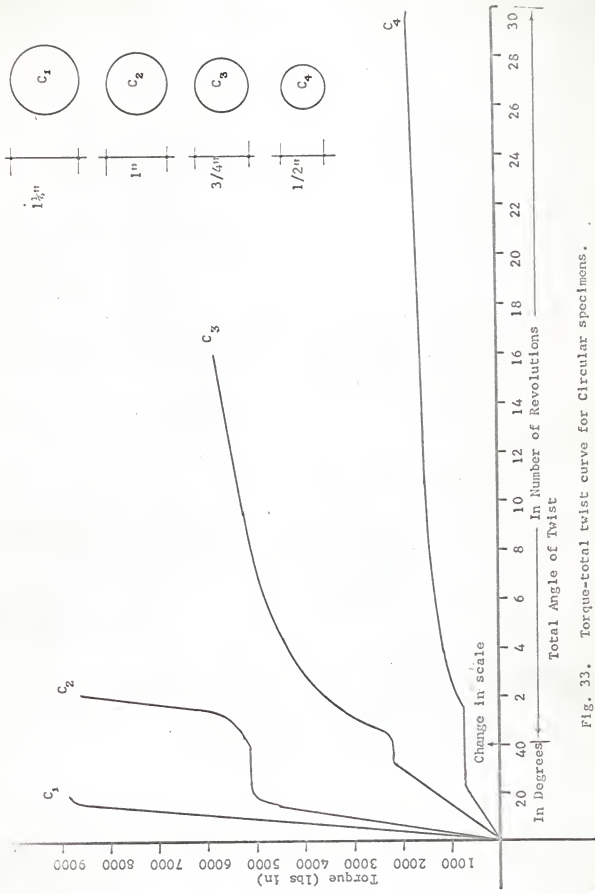


Fig. 33. Torque-total twist curve for Circular specimens.

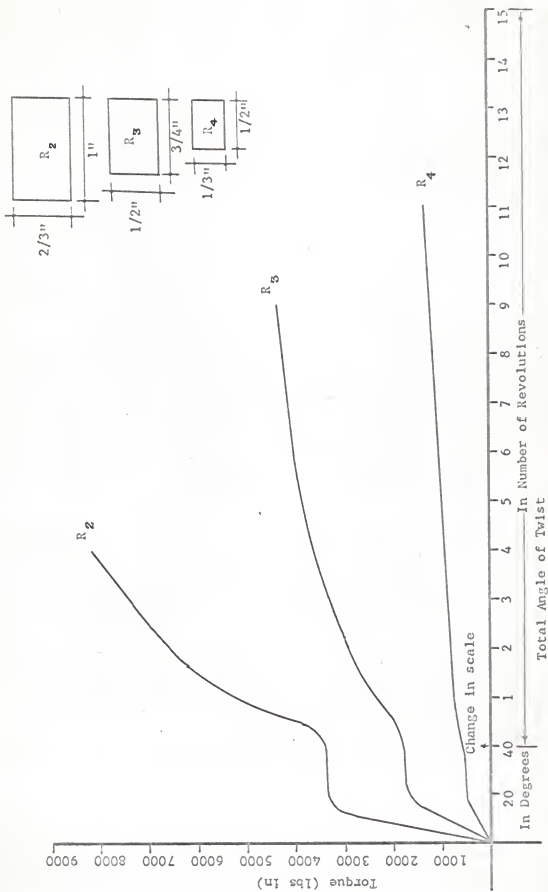


Fig. 34. Torque-total twist curve for Rectangular specimens (b/a=1.5).

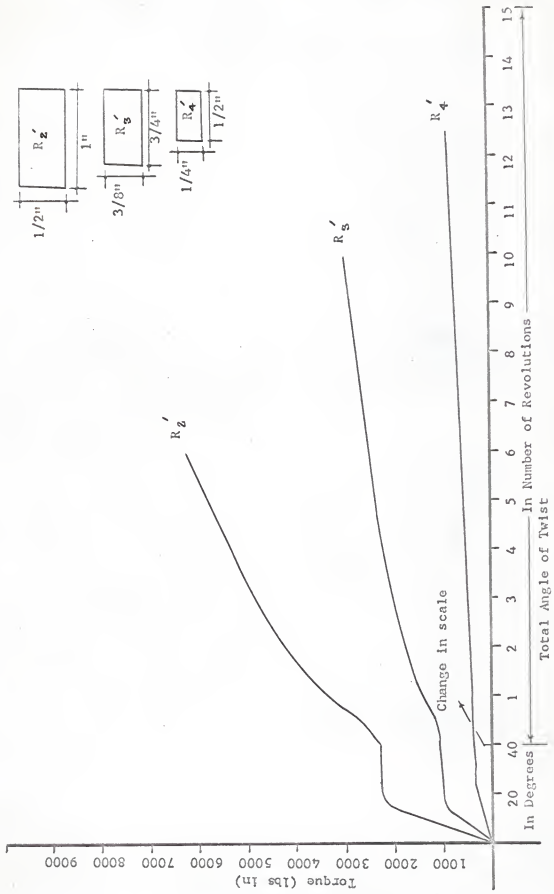


Fig. 35. Torque-total twist curve for Rectangular specimens ($b/a=2.0$).

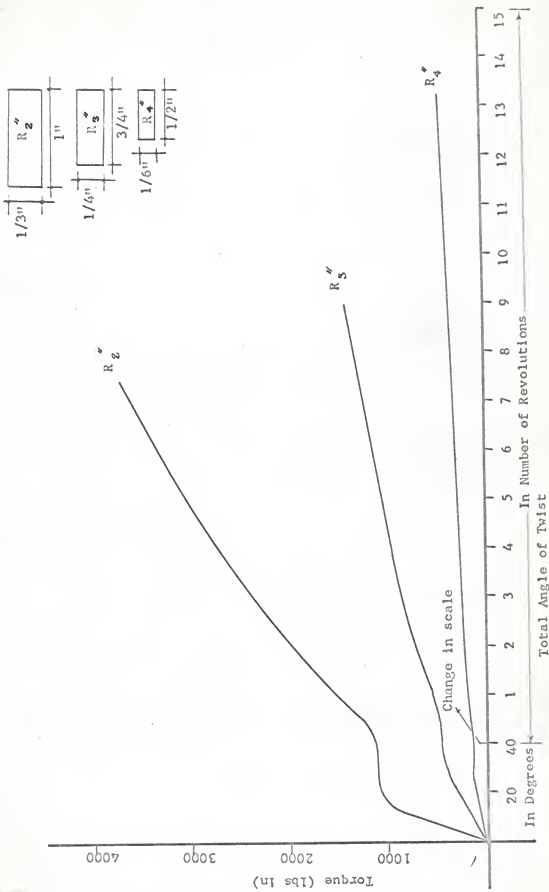


Fig. 36. Torque-total twist curve for Rectangular specimens ($b/a=3.0$).

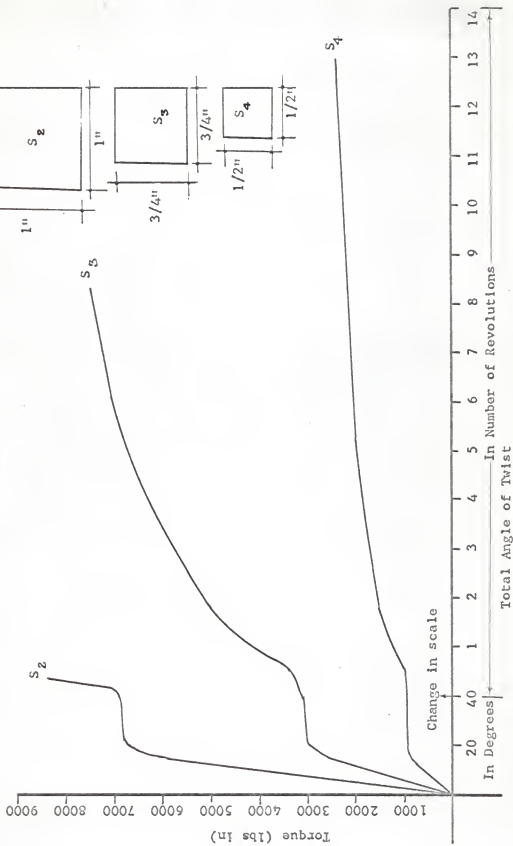


Fig. 37. Torque-total twist curve for Square specimens.



Fig. 38 Fractured circular specimens.



Fig. 39 Fractured rectangular specimens ($b/a=1.5$).



Fig. 40 Fractured rectangular specimens ($b/a=2.0$)



Fig. 41 Fractured rectangular specimens ($b/a=3.0$).



Fig. 42 Fractured square specimens.

Table 7. Torsional properties.

No.	Specimen No.	Modulus of Shear (From Torque-Twist Curve)	Theoretical Yield Torque (lb in)	Theoretical Fully Plastic Torque (lb in)	Remarks
1	C ₁	11.0 x 10 ⁶	8270	11,000	Specimen did not break due to limited capacity of machine.
2	C ₂	11.9 x 10 ⁶	14250	5670	do.
3	C ₃	11.7 x 10 ⁶	1845	2460	Fracture at left grip.
4	C ₄	10.9 x 10 ⁶	610	812	do.
5	R ₂	11.1 x 10 ⁶	2300	3720	Specimen did not break due to limited capacity of machine.
6	R ₃	11.1 x 10 ⁶	1290	2120	Fracture at right grip.
7	R ₄	11.8 x 10 ⁶	394	679	do.
8	R ₂ '	10.9 x 10 ⁶	1405	2340	Fracture at left grip.
9	R ₃ '	11.8 x 10 ⁶	761	1285	Fracture at right grip.
10	R ₄ '	11.1 x 10 ⁶	204	345	Fracture at left grip.
11	R ₂ "	10.9 x 10 ⁶	635	1140	Fracture at right grip.
12	R ₃ "	12.3 x 10 ⁶	299	495	do.
13	R ₄ "	11.5 x 10 ⁶	97	163	Fracture at left grip.
14	S ₂	12.4 x 10 ⁶	4630	7540	Specimen did not break due to limited capacity of machine.
15	S ₃	11.9 x 10 ⁶	2300	3630	Fracture at left grip.
16	S ₄	12.1 x 10 ⁶	660	1050	Fracture at right grip.

behaviour depends primarily on the rate of change of the elastic portion in the cross section to the plastic state, and since this rate is low in the case of non-circular cross sections, the transition of torque-twist curve is quite gradual. (Refer to Fig. 11).

4.3 TORQUE-STRESS CURVE

As mentioned in the previous chapter, torque-stress relationships were experimentally determined for specimens R_2 , R_2' , R_2'' and S_2 , and the torque-stress curves are shown in Fig. 43.

Discussing again specimen R_2' , the strain readings are obtained from Table 6. The strains were measured in three directions inclined 120° to each other. To determine the principal strain, Mohr's circle for strain was constructed as shown in Fig. 44.

$$\epsilon_1 = 2648 - 2653 = -5 \times 10^{-6}$$

$$\epsilon_2 = 2250 - 3110 = -860 \times 10^{-6}$$

$$\epsilon_3 = 1038 - 200 = +838 \times 10^{-6}$$

$$m = \frac{1}{3} (\epsilon_1 + \epsilon_2 + \epsilon_3)$$

$$= \frac{1}{3} (-5 - 860 + 838)$$

$$= -9$$

$$Oa = \epsilon_1 - m = -5 + 9 = +4 \times 10^{-6}$$

$$Ob = \epsilon_2 - m = -860 + 9 = -851 \times 10^{-6}$$

$$Oc = \epsilon_3 - m = +838 + 9 = +847 \times 10^{-6}$$

$$R_\epsilon \text{ (from Fig. 44)} = 980 \times 10^{-6}$$

$$R_s = R_{\epsilon_{1+u}} \frac{E}{1+\mu}$$

$$= 980 \times 10^{-6} \frac{31.0 \times 10^6}{1.281}$$

$$= 23,700 \text{ psi}$$

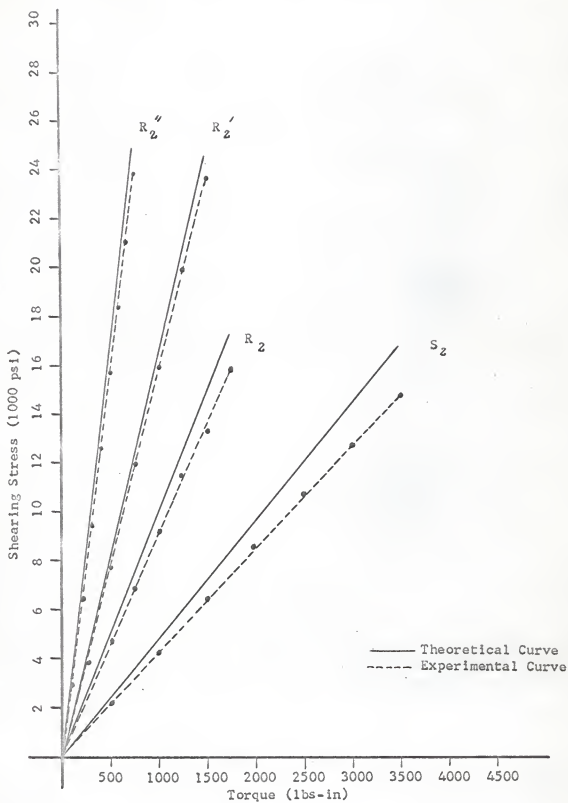


Fig. 43. Shearing stress-torque curves.

The radius of the strain circle was found to be 980×10^{-6} , which is the required principal strain. The maximum shearing stress is represented by the radius of the Mohr's stress circle. This value can be determined from the Mohr's strain circle by the formula

$$R_s = R \frac{E}{1 + \mu}$$

The experimental values of the maximum shearing stress were determined for convenient intervals of torque and are plotted in Fig. 43. The theoretical torque-stress curve in the figure was drawn from the theoretical values obtained for maximum shearing stress by using the torque-stress formula for a rectangular cross section ($\frac{b}{a} = 1.5$). This calculation is explained in detail in the next section.

4.4 CORRELATION OF THEORETICAL AND EXPERIMENTAL TORQUES

The formulas for computing theoretical torques have been discussed in chapter 2. It was also pointed out that the torque-yield stress relationship can be deduced very easily for the circular and square cross sections. The formula for a rectangular cross section (Eq. 25) was presented in a generalized form due to the unknown ratio of the sides of the rectangular cross sections. The formulas for rectangular sections are now derived for each particular side ratio.

$$\begin{aligned} \frac{b}{a} &= 1.5 \\ \tau_{\max} &= 2G\theta a - \frac{16G\theta a}{\pi^2} \sum_{n=1, 3, 5, \dots}^{\infty} \frac{1}{n^2 \cosh \frac{n\pi b}{2a}} \\ &= 2G\theta a \left\{ 1 - \frac{8}{\pi^2} \left(\frac{1}{\cosh 2.36} - \dots \right) \right\} \\ &= 2G\theta a \left(1 - \frac{8}{\pi^2 \times 5.343} \right) \\ &= 2G\theta a (1 - 0.152) \end{aligned}$$

$$= 2G \ a \times 0.848 = 1.696 \ G \ a$$

$$T_e = \frac{1}{3} G \ (2a)^3 (2b) \left[1 - \frac{192}{5} \frac{a}{b} x \right]_{n=1, 3, 5} - \frac{1}{n^5} \tanh \frac{n}{2a} b$$

$$= \frac{24}{3} G \ a^4 \left[1 - \frac{128}{5} \tanh 2.36 \right]$$

$$= 8G \ a^4 \left[1 - \frac{128}{5} \times 0.982 \right]$$

$$= 8G \ a^4 (1 - 0.11)$$

$$= 4.72 \ G \ a^4$$

$$= \frac{4.72}{1.696} \ a^3$$

$$= 2.78 \ a^3$$

$$\frac{b}{a} = 2.0$$

$$\max = 2G \ a \left[1 - \frac{8}{2} \left(\frac{1}{\cosh} + \frac{1}{9 \cosh} + \dots \right) \right]$$

$$= 2G \ a \left[1 - \frac{8}{2} \left(\frac{1}{11.6} + \frac{1}{9 \times 6300} \right) \right]$$

$$= 2G \ a \left(1 - \frac{8}{2 \times 11.6} \right)$$

$$= 2G \ a (1 - 0.068)$$

$$= 1.864 \ G \ a$$

$$T_e = \frac{32}{3} G \ a^4 \left[1 - \frac{96}{5} x \right]_{n=1, 3, 5} - \frac{1}{n^5} \tanh n$$

$$= \frac{32}{3} G \ a^4 \left[1 - \frac{96}{5} (0.996 + 0.00111) \right]$$

$$= \frac{32}{3} G \ a^4 (1 - 0.31)$$

$$= 7.35 \ G \ a^4$$

$$= \frac{7.35}{1.864} \ a^3$$

$$= 3.94 \ a^3$$

$$\frac{b}{a} = 3.0$$

$$\begin{aligned} \tau_{\max} &= 2G\theta a \left\{ 1 - \frac{8}{\pi^2} \left(\frac{1}{\cosh 4.71} + \frac{1}{9 \cosh 11.12} + \dots \right) \right\} \\ &= 2G\theta a \left\{ 1 - \frac{8}{\pi^2} \left(\frac{1}{54.97} + \dots \right) \right\} \\ &= 2G\theta a (1 - 0.0148) \\ &= 2G\theta a \times 0.986 = 1.972G\theta a \end{aligned}$$

$$\begin{aligned} T_o &= \frac{1}{5} G\theta 8a^3 2b \left\{ 1 - \frac{64}{\pi^5} (\tan h 4.71 + \dots) \right\} \\ &= 16G\theta a^4 \left(1 - \frac{64}{\pi^5} \times 0.999 \right) \\ &= 16G\theta a^4 (1 - 0.21) \\ &= 16G\theta a^4 \times 0.79 \\ &= 12.66 G\theta a^4 \\ &= \frac{12.66}{1.972} \tau_{a3} a^3 = 6.42 \tau_{a3} a^3 \end{aligned}$$

The yield torques and the plastic torques calculated from these formulas for all the specimens have been summarized in Table 7. These values have also been indicated in the torque-twist diagrams. (Refer to Figs. 25 to 32) These figures indicate that the calculated yield torque was below the experimental value in all cases, while the calculated plastic torque was higher than the experimental value in each test.

The under estimation of the yield torque is due to the fact that a slight increase in the yielded zone at the periphery of the cross section does not effect the rate of increase of torque, that is, the slope of the torque-twist

curve, and therefore the elastic-plastic torque still seems to be in the elastic range.

The plastic torque is defined as the torque which causes the entire cross section to become plastic. This stage comes after considerable deformation of the specimen, especially along the diagonals of the square and rectangular cross sections. During this deformation, strain-hardening starts for portions which became plastic first. The calculated plastic torque is therefore located on that portion of torque-twist curve where strain-hardening starts occurring.

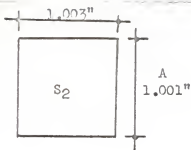
In short, it may be said that the theoretical yield torque is lower than the experimental value, whereas the theoretical plastic torque is higher than that indicated on the experimental torque-twist curve.

4.5 CORRELATION OF THEORETICAL AND EXPERIMENTAL SHEAR STRESSES

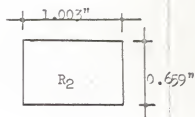
It was known before starting this investigation that the experimentally determined shearing stress would not be very precise. There ought to be a difference between the theoretical shearing stress and the experimental shearing stress (obtained from Mohr's circle) because the size of the strain rosettes was too large to measure the strain precisely at the center of the greater side of the rectangular and square cross sections. The strain rosettes were applied on the one inch sides of each of the four specimens. The shearing stress is a maximum at the centers of these sides, but it is zero at points only one half inch away from the center, that is, at the corners. The strain rosettes were measuring strains at points slightly away from the center, resulting in a smaller value of the maximum shearing stress.

The experimental shearing stresses were determined for each specimen as explained in Sec. 4.3 and the values have been summarized in Table 8.

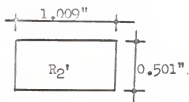
A graph of shearing stresses versus torque has been plotted in Fig. 43 for each cross section. The dotted curve is plotted from the experimental shearing



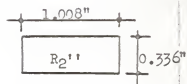
Torque (lb in)	Shearing Stress (psi)
500	2130
1000	4320
1500	6450
2000	8540
2500	10,690
3000	12,780
3500	14,850



Torque (lb in)	Shearing Stress (psi)
250	2,270
500	4,640
750	6,950
1000	9,240
1250	11,500
1500	13,300
1750	15,920



Torque (lb in)	Shearing Stress (psi)
250	3,880
500	7,900
750	12,000
1000	15,900
1250	19,990
1500	23,800
1720	27,200
1930	31,200
2045	42,500



Torque (lb in)	Shearing Stress (psi)
100	3,160
200	6,350
300	9,400
400	12,680
500	15,800
580	18,400
675	21,550
770	24,600
860	28,100

Table 8. Experimental Shearing Stress.

stress values obtained from Table 8, and the solid curve is obtained from the theoretical shearing stress values deduced from formulas, explained in Sec. 4.4.

The difference between the theoretical and the experimental shearing stress for all the four cross sections is due to the inability of the strain rosettes to measure strains exactly at the centers of the sides, as previously explained.

5 CONCLUSIONS

The following conclusions are based on the foregoing theoretical and experimental investigations for solid prismatic members subjected to elastic and plastic torsion:

(1) The experimentally measured elastic torques were somewhat higher than the theoretical maximum elastic torques, whereas the experimental plastic torques were slightly lower than the theoretical plastic torques.

(2) For the same cross-sectional area, circular members can sustain a higher total angle of twist than non-circular members for the same loading.

(3) Strain hardening in specimens subjected to torsional loading starts before the entire cross section becomes plastic.

(4) In the case of non-circular members, those having a higher width-depth ratio exhibit a greater torsional strength for the same area of cross section.

(5) In the elastic range, the maximum shearing strength varies linearly with the applied torque.

(6) For the same torque, the experimental shearing stress in a specimen was found to be lower than the theoretical shearing stress. This was due to the fact that with the use of large size rosettes it was not possible to measure the shearing stress precisely at the center of the side.

6 RECOMMENDATIONS FOR FURTHER RESEARCH

It would be interesting to analyse the elastic-plastic boundary changes with increasing torque for a given cross section. The best known analytical solution is for an oval cross section, which was originally presented by Sokolovsky. An experimental method for obtaining a solution of the elastic-plastic torsion problem has been developed by Nadai (discussed in Chapter 2).

Another possible investigation would be to determine the torque for a finite angle of twist, taking strain hardening into consideration.

7 ACKNOWLEDGEMENT

The author wishes to express his sincere gratitude and appreciation to his major Professor, Dr. Peter B. Cooper, for his guidance and encouragement throughout this study, and for his valuable assistance, criticism and advice during the preparation of the thesis.

Sincere thanks are extended to Dr. Jack B. Blackburn, Prof. Vernon H. Rosebraugh, and Dr. Edwin C. Lindly, members of the advisory committee, for their supervision and valuable suggestions.

Thanks are also due to Mr. Wallace M. Johnston for his assistance in the experiments.

The author wishes to express his indebtedness to his parents for their encouragement and patience during the period of this study.

8 REFERENCES

1. Coulomb, Histoire de L'academie, 1784, Paris.
2. Navier (Edited by Saint Venant), Resume des lecons sur l'application de La mecanique, 1864, Paris.
3. Saint Venant, Mem acad sci savants etrangers, 1855, Vol. XIV.
4. Tresca, Mem presentes par divers savants, 1859, Vol. 20.
5. Timoshenko, Stephen P., History of Strength of Materials, 1953, McGraw-Hill Book Co., Inc.
6. Nadai, A., Plasticity, 1931, McGraw-Hill Book Co., Inc.
7. Prager, W. and P. G. Hodge, Theory of Perfectly Plastic Solids, 1951, John Wiley & Sons, Inc.
8. Johnson, W. and P. G. Mellor, Plasticity for Mechanical Engineers, 1961, D. Van Nostrand Co., Inc.
9. Timoshenko, S. and G. H. MacCullough, Elements of Strength of Materials, 1949, D. Van Nostrand Co., Inc.
10. Prandtl, L., Sur torsion von prismatischen staeben, 1903, Phys. Z 4.
11. Timoshenko, S., Theory of Elasticity, 1934, McGraw-Hill Book Co., Inc.
12. Clark, D. A. R., Advanced Strength of Materials, 1951, Blackie & Smith.
13. Hodge, P. G., Jr., Plastic Analysis of Structures, 1959, McGraw-Hill Book Co., Inc.
14. Marin, J. and J. A. Sauer, Strength of Materials, 1954, MacMillian Co.
15. Singer, Gerdinand L., Strength of Materials, 1962, Harper and Row Co.
16. Seely, Fred B. Resistance of Materials, 1925, John Wiley and Sons, Inc.
17. Popov, E. P., Mechanics of Materials, 1943, Prentice-Hall, Inc.
18. Hartog, J. P. Den., Advanced Strength of Materials, 1952, McGraw-Hill Book Co., Inc.
19. Proceedings of the American Society for testing materials, Twenty eighth annual meeting, Vol. 25, 1925. Part I Committee Reports.
20. AST M Standards, Part 4, Jan. 1966.
21. AST M Standards, Part 31, May 1967.

22. Yarnell, J., Resistance Strain Gages, Electronic Engg., Aug. 1951.
23. Proceedings of the American Society for testing materials, Forty first annual meeting, Vol. 38, 1938. Part II, Technical papers.
24. Proceedings of the American Society for testing materials, Thirty third annual meeting, Vol. 30, 1930. Part II, Technical papers.
25. AST M Standards, Part 3, November, 1958.
26. Hetenyi, M., Handbook of Experimental Stress Analysis, Vol. XII, No. 1, 1950 John Wiley, and Sons, Inc.
27. "Symposium on Shear and Torsion Testing", AST M Special Technical Publication No. 289, February, 1961.
28. "Length changes in Metals under Torsional overstrain", Engineering, Vol. 163, 1947.
29. Smith, J. O. and O. M. Sidebottom, Inelastic behaviour of load-carrying members, 1965, John Wiley and Sons, Inc.

THE STRENGTH OF SOLID PRISMATIC
MEMBERS IN TORSION

by

HASEEB AHMED KHAN

B. E. (Civil), University of Karachi, Karachi, 1966

AN ABSTRACT OF A MASTER'S THESIS

submitted in partial fulfillment of the

requirements for the degree

MASTER OF SCIENCE

Department of Civil Engineering

KANSAS STATE UNIVERSITY
Manhattan, Kansas

1969

The purpose of this study was to study experimentally the behaviour of solid prismatic bars under elastic and plastic torsion, and to compare the experimental results with existing analytical solutions. The study was limited in scope to solid prismatic steel members subjected to pure torsion.

The data were collected for four circular, nine rectangular and three square cross sections. The nine rectangular specimens were divided into three groups, each having a different width-depth ratio.

In order to calculate theoretical values for the test specimens, coupon tests were conducted to determine the yield strength, modulus of elasticity and Poisson's ratio. The theoretical torques and shear stresses were based on these properties.

From the torsion tests, torque-twist curves were drawn for each specimen. The results indicated that the theoretical yield torques were somewhat lower than the experimental yield torques. Unlike a stress-strain curve, the transition from elastic to plastic behaviour was very gradual. For the same area of cross section, the torsional strength of the rectangular specimens increased with an increase in the width-depth ratio.

Maximum shearing stresses were experimentally determined for three rectangular and one square cross section. The strains were measured from strain rosettes and then maximum shearing stresses determined by constructing Mohr's circle. The experimental shearing stresses thus determined was found to be lower than the theoretical shearing stresses.